Clim Dyn
DOI 10.1007/s00382-007-0344-8

Coupled North Atlantic slope water forcing on Gulf of Maine temperatures over the past millennium

Alan D. Wanamaker Jr · Karl J. Kreutz · Bernd R. Schöne · Neal Pettigrew · Harold W. Borns · Douglas S. Introne · Daniel Belknap · Kirk A. Maasch · Scott Feindel

Received: 26 March 2007 / Accepted: 15 November 2007

Abstract To investigate ocean variability during the last millennium in the Western Gulf of Maine (GOM), we collected a 142-year-old living bivalve (*Arctica islandica* L.) in 2004, and three fossil *A. islandica* shells (calibrated $^{14}C_{AMS}$ = 1030 ± 78 AD; 1320 ± 45 AD; 1357 ± 40 AD) for stable isotope and growth increment analysis. A statistically significant relationship exists between modern GOM temperature records [shell isotope-derived (30 m) ($r = -0.79$; $P < 0.007$), Prince 5 (50 m) ($r = -0.72$; $P < 0.019$), Boothbay Harbor SST ($r = -0.76$; $P < 0.011$)], and Labrador Current (LC) transport data from the Eastern Newfoundland Slope during 1993–2003. In all cases, as LC transport increased, GOM water temperatures decreased the following year. Decadal trends in the North Atlantic Oscillation (NAO) and the Atlantic Multidecadal Oscillation (AMO) influence GOM water temperatures in the most recent period, with water temperatures decreasing during NAO and AMO negative modes most likely linked to LC transport and Gulf Stream interaction. Mean shell-derived isotopic changes ($\delta^{18}O_c$) during the last 1,000 years were +0.47‰ and likely reflect a 1–2°C cooling from 1000 AD to present. Based on these results, we suggest that observed cooling in the GOM during the last millennium was due to increased transport and/or cooling of the LC, and decreased Gulf Stream influence on the GOM.

A. D. Wanamaker Jr · K. J. Kreutz · H. W. Borns · D. S. Introne · D. Belknap · K. A. Maasch
Climate Change Institute and Department of Earth Sciences, University of Maine, Orono, ME 04469-5790, USA

A. D. Wanamaker Jr (✉)
School of Ocean Sciences, University of Wales at Bangor, Menai Bridge, Anglesey LL59 5AB, UK
e-mail: oss609@bangor.ac.uk

B. R. Schöne
Increments Research Group, Department of Paleontology, Institute of Geosciences, University of Mainz, Johann-Joachim-Becher-Weg 21, 55128 Mainz, Germany

N. Pettigrew
School of Marine Sciences, University of Maine, Orono, ME 04469-5790, USA

S. Feindel
Darling Marine Center, University of Maine, Walpole, ME 04573, USA

1 Introduction

The oceanography along the slope of the Eastern Canadian coast and the deep Gulf of Maine (GOM) is strongly influenced by the position, strength, and properties of the Labrador Current (LC) (Fig. 1). The LC has two distinct branches of flow: the principal branch that flows generally southward along the continental slope, and an inner branch that flows over the Labrador and Newfoundland continental shelf regions (Lazier and Wright 1993). At times, water of LC origin extends from the western Labrador Sea to the Middle Atlantic Bight (e.g., Petrie and Drinkwater 1993; Loder et al. 2001), and has a net cooling effect on both air and coastal water temperatures along the Canadian Atlantic provinces (e.g., Drinkwater et al. 1999). Han and Li (2004) estimated an annually averaged flow of ~6 Sv (1 Sv = 10^6 m^3 s^{-1}) for the LC along the Eastern Newfoundland Slope (200–3,000 m) using TOPEX/Poseidon satellite altimeter data (Fig. 1). Gatien (1976) identified two types of slope waters outside the GOM and along the Scotian Shelf, Labrador Slope Water (LSW) and Warm Slope Water (WSW). From the Labrador Sea, the cold,

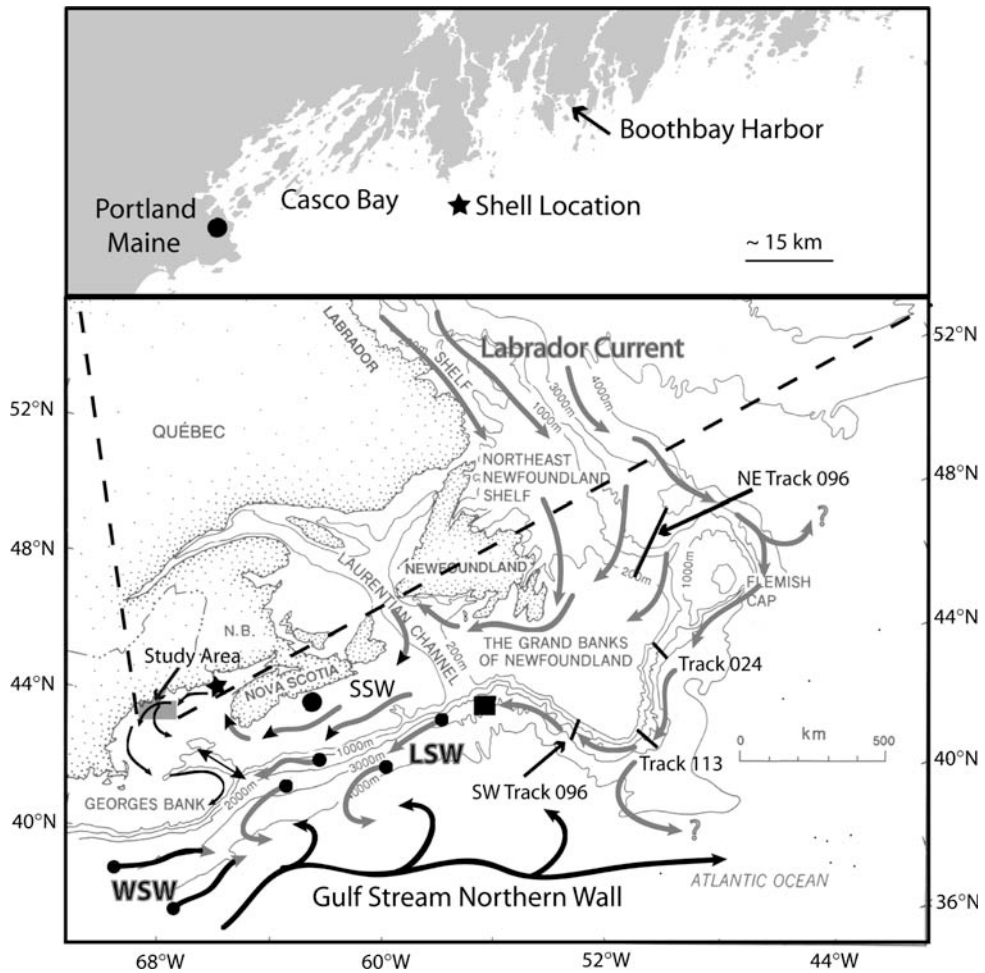

Fig. 1 The general bathymetric map and surface circulation for the Gulf of Maine (GOM) region (fine *black line* within the GOM) and Eastern Canada, noting long-term climate stations [Portland (air temperature); Boothbay Harbor (SST)] and the shell collection location in the Western Gulf of Maine (*top*) are shown. Within the Northeastern Gulf of Maine (*bottom*) is the Prince 5 station (50 m water temperature and salinity data; *filled star*). The approximate Labrador Current transects (NE Track 096; Track 024; Track 113; SW Track 096) located along the Newfoundland Slope of Han and Li (2004) are illustrated. The locations for the studies of Keigwin et al. (2003) (Emerald Basin, off Nova Scotia; *filled circle*) and Marchitto and deMenocal (2003) (located south of Newfoundland and the Grand Banks; *filled square*) are shown. Major ocean currents and water masses for the region are shown with their approximate locations and patterns [Labrador current (LC; *gray line* and *arrow*), Scotian Shelf Water (SSW; *gray line with black arrow*), Labrador Slope Water (LSW; *gray with black circle*), Warm slope water (WSW; *black line and circle with gray arrow*), Gulf Stream (*black line and arrow*)]. Map was modified from Keen and Piper (1990)

relatively fresh and nutrient-poor water masses of the southward flowing LSW mix with the warm, relatively saline and nutrient-rich waters of the WSW (Gulf Stream-derived) moving northward (Lazier and Wright 1993; Drinkwater et al. 1999; Petrie and Yeats 2000). Further, Gatien (1976) suggested that the slope water properties for the region depend upon whether the LSW or WSW component is dominant. Petrie and Drinkwater (1993) postulated that oceanographic conditions in the GOM and along the Scotian Shelf partly reflect the penetration of slope waters onto the shelf in the deep layers through gullies and channels, related to meteorological events, Gulf Stream activity (rings), or gravitational flows generated by differences in the density of the water on and off the shelf.

In addition to several large rivers (St John, Penobscot, Kennebec, and Androscoggin), the freshwater budget for the GOM is significantly controlled by the inflow of Scotian Shelf Water (SSW) (Smith 1983; Brown and Irish 1993), a water mass that is characterized as relatively cold and with low salinity (e.g., Pettigrew et al. 1998). Scotian Shelf Water is a mixture of water from the Labrador and Newfoundland shelf regions, as well as water from the Gulf of St. Lawrence (e.g., Houghton and Fairbanks 2001). Scotian Shelf Water flows southward along the continental shelf of Nova Scotia and into the GOM.

Dominant modes of atmospheric and oceanic variability such as the North Atlantic Oscillation (NAO) and the Atlantic Multidecadal Oscillation (AMO) have been linked

to environmental change in the North Atlantic and surrounding regions (e.g., Hurrell 1995; Enfield et al. 2001; Drinkwater et al. 2003; Sutton and Hodson 2003, 2005; Knight et al. 2005, 2006). North Atlantic Oscillation forcing has been linked to LC transport variability (e.g., Myers et al. 1989; Dickson et al. 1996; Marsh et al. 1999), the position of the northern Gulf Stream wall (Taylor and Stephens 1998), and certain zooplankton levels in the Gulf of Maine (e.g., Conversi et al. 2001; MERCINA 2001; Greene and Pershing 2003). In an NAO low mode (weaker westerlies over the Labrador Sea and North Atlantic) there is decreased winter heat loss, decreased winter storminess, and suppressed ocean convection in the Labrador Sea (rarely reaching deeper than 1,000 m) (Dickson et al. 1996). These conditions, along with a greater input of relatively fresh polar waters via the East Greenland Current, are thought to lead to an increased buildup of fresh surface water in the Labrador Sea, and increased buoyancy-driven LC transport (Dickson et al. 1996). A persistent NAO low pattern may cause GOM water temperatures to decrease for two reasons: (1) increased LSW water would likely enter the GOM (e.g., MERCINA 2001), and (2) a southward displacement of the northern wall of the Gulf Stream would allow decreased transport of WSW to enter the GOM.

The AMO is a measure of SST temperature anomalies in the North Atlantic in part related to thermohaline circulation (THC) with a periodicity of $\sim$70 years (e.g., Delworth and Mann 2000; Sutton and Hodson 2005). The AMO has been associated with precipitation patterns in the United States and Western Europe (e.g., Enfield et al. 2001), winter air temperatures in Europe (Folland et al. 1986), and Atlantic hurricane formation (Goldenberg et al. 2001). Dima and Lohmann (2007) recently suggested that the dynamics of the AMO are governed by interactions and feedbacks among the ocean, atmosphere, and sea ice. In the mechanistic model of Dima and Lohmann (2007), increased THC strength induces North Atlantic and North Pacific SST anomalies, which in turn impact sea level pressure (SLP) fields in the North Atlantic and North Pacific. The resulting SLP fields and associated wind stress modifies the export of sea ice and freshwater from the Fram Strait into the North Atlantic, ultimately affecting meridional overturning circulation (MOC) (see Dima and Lohmann 2007 for a detailed description). Although the relationship between Gulf Stream transport and the AMO is still poorly understood, it is plausible that decadal-to-multidecadal changes in the MOC and Gulf Stream transport would cause SST anomalies in the North Atlantic (e.g., Delworth and Mann 2000), and possibly within the GOM. However, the relationships among dominant climate modes (NAO and AMO), slope water currents, and water temperatures in the GOM are poorly understood over the past millennium. Because observational records of temperature and salinity for the GOM are spatially and temporally limited, marine-based proxy records can significantly extend our knowledge of past ocean conditions.

Oxygen isotopes ($\delta^{18}O_c$) from the shells of the bivalve *A. islandica* (Linnaeus 1767) (ocean quahog) have been used extensively in paleoceanography (Weidman and Jones 1993; Weidman et al. 1994; Marsh et al. 1999; Schöne et al. 2004; 2005a, b). Weidman et al. (1994) concluded that *A. islandica* precipitates its aragonitic shell ($\delta^{18}O_c$) in isotope equilibrium with ambient seawater, thus water temperature estimates can be made when the isotopic composition of the water ($\delta^{18}O_w$) is known or can be estimated ($\delta^{18}O_w$—related to salinity). The ocean quahog is a slow-growing bivalve that commonly lives more than 100 years (e.g., Ropes and Murawski 1983; Forsythe et al. 2003; Schöne et al. 2005a) with a sub-arctic to mid-latitude distribution in the North Atlantic (Cargnelli et al. 1999). Because *A. islandica* deposits distinct annual lines in its shell, it is possible to reconstruct past ocean environments at sub-annual to annual resolution (Thompson et al. 1980; Jones 1983; Ropes et al. 1984), and if the collection date is known, paleoenvironmental reconstructions with an absolute chronology can be constructed (e.g., Jones 1983). Our goals in this paper are to (1) use both modern and $^{14}C_{AMS}$ dated fossil *A. islandica* shells to document ocean variability during the late Holocene in the Western Gulf of Maine, (2) identify possible local and regional scale mechanisms responsible for the shell-derived isotope time-series based on comparisons with instrumental data from the GOM and the North Atlantic, and (3) estimate the influence of North Atlantic atmospheric and oceanic variability on GOM oceanography over the past millennium.

2 Experimental methods

2.1 Sample collection

One specimen of *A. islandica* was collected alive in the Western Gulf of Maine, USA (43° 39′ 22.14″ N, 69° 48′ 6.01″ W), in 30 m water depth via the fishing vessel FV Foxy Lady on March 14, 2004 during a Maine Department of Marine Resources dredge survey (Fig. 1). Three well-preserved articulated fossils of *A. islandica* were collected 3 km away (43° 41′ 13.14″ N, 69° 47′ 56.34″ W) in 38 m water depth via a Rossfelder vibracore (SBVC-9609) on September 29, 1996 (Fig. 1). There was no evidence of diagenesis (e.g., opaque rims or alteration from aragonite to calcite) in any shell used in this study.

2.2 Sclerochronological and isotope analyses

In preparation for sclerochronological and isotope analyses, we used methods outlined by Schöne et al. (2005a).

The left valve from each shell was mounted on a plexiglass block, and a quick-drying metal epoxy resin (JB KWIK-Weld) was then applied to the surface (inside and out). Two thick sections (3 mm) of shell were cut from the valve along the axis of maximum growth, and perpendicular to the annual growth lines with a Buehler Isomet low-speed saw using a 0.3 mm thick diamond wafering blade. Each section was mounted on a glass slide, ground with 800 and 1,200 SiC grit, polished with 1 μm Al_2O_3 powder and cleaned with dehydrated ethyl alcohol. Further, to resolve annual growth patterns (sclerochronology), one polished section from each shell was immersed in Mutvei's solution for 20 min at ~38°C. The treated shell was immediately rinsed with demineralized water and air-dried. The growth patterns of the etched shell were viewed under a reflected light stereomicroscope (Leica Wild M3Z) and digitized using a Nikon Coolpix 995 camera. Annual growth widths were determined to the nearest 1 μm with Scion Image (version 1.63). Measurements were conducted on the outer shell surface.

Carbonate samples were micromilled along annual growth increments from the untreated shell section after Schöne et al. (2005a). Annual oxygen isotope values ($\delta^{18}O_c$) (autumn to autumn) were calculated by averaging sub-annual $\delta^{18}O_c$ samples for each year. Based on approximately 3,000 $\delta^{18}O_c$ analyses on the four shells, the average number of sub-annual $\delta^{18}O_c$ samples per year was ~8 (range 1–54). Each aragonitic carbonate sample weighed ~50 μg. The samples were reacted with 99% anhydrous phosphoric acid at 72°C in an automated carbonate preparation device (Gas Bench II) coupled to a Finnigan MAT-253 continuous-flow mass spectrometer at the University of Frankfurt, Germany. Oxygen and carbon isotope ratios of the samples are reported in per mil units (‰) relative to the VPDB (Vienna Pee-Dee Belemnite) carbonate standard based on a NBS-19 calibrated Carrara marble value of −1.76‰ ($\delta^{18}O_c$) and +2.02‰ ($\delta^{13}C_c$). Precision of the instrument determined from replicate analyses was ±0.07‰ for $\delta^{18}O$ and ±0.05‰ for $\delta^{13}C$.

2.3 Calculation of sea water temperatures and shell $^{14}C_{AMS}$ dating

We used the modified Grossman and Ku (1986) aragonite equation (Eq. 1) with the Houghton and Fairbanks (2001) GOM isotope/salinity mixing line from the Northeast Channel (Eq. 2) to calculate annual water temperatures, which are shown below [$\delta^{18}O_c$‰ (VPBD); $\delta^{18}O_w$‰ (Vienna Standard Mean Ocean Water; VSMOW)]:

$$T(^{\circ}C) = 20.60 - 4.34 \times \left(\delta^{18}O_c\left(\delta^{18}O_w - 0.20\right)\right), \quad \text{and} \tag{1}$$

$$\delta^{18}O_w(\text{VSMOW}) = (0.57 \times \text{Salinity}) - 19.50. \tag{2}$$

Salinity values were available (see below) from 1928–present (Fig. 2). Prior to 1928, salinity (practical salinity units; PSU) was estimated based on the long-term mean at the Canadian Prince 5 station (32.1 ± 0.22 PSU) to calculate annual water temperatures. $^{14}C_{AMS}$ dating was used to determine the approximate calendar age of the ventral margin (oldest part of the shell, but youngest with respect to ^{14}C). Calibrated ^{14}C ages (cal year AD) were calculated using Calib 5.01 (Stuiver and Reimer 1993) using a regional GOM marine reservoir effect of $\Delta R = 39 \pm 40$ (Tanaka et al. 1990), which included quahog shells (*A. islandica* and *Merceneria mercenaria*) from museum collections. The calendar age assigned to the entire shell resulted from counting the annual growth layers (Jones 1983) from the ventral margin back to the umbo region.

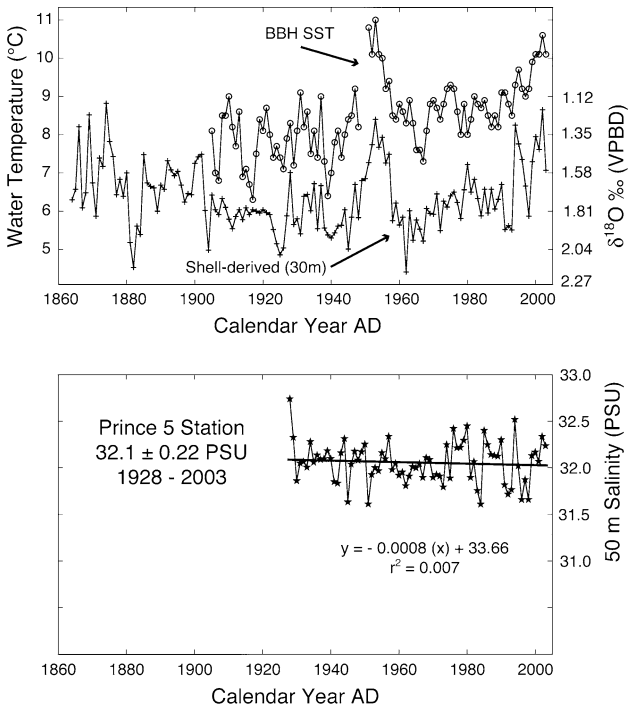

Fig. 2 *Top* Annual shell isotope-derived (30 m) water temperature (*plus sign*) and annual BBH SST record (*open circles*) (Lazzari 2001) are illustrated. The annual linear correlation (*r*) between the records from 1905 to 2003 is $r = 0.71$ ($P < 0.0001$). Shell-derived water temperature estimates from 1928 – 2003 are based Prince 5 (50 m) salinity values (*bottom*). Prior to 1928, shell-derived water temperature estimates are based on the long-term mean salinity values (32.1 ± 0.22 PSU) from Prince 5. The salinity trend at Prince 5 (50 m) is not statistically significant

2.4 Instrumental data

Instrumental data used in this paper includes air temperatures from Portland, Maine (National Climate Data Center; 1895–present), SST from Boothbay Harbor (Lazzari 2001) (1905–present), and 50 m water temperature and salinity values from Prince 5 station (1928–present) (Fig. 1). It should be noted that monthly, long-term (>50 years) salinity measurements in the GOM are only available from the Prince 5 station. We used a winter (DJFM) NAO index (NOAA Climate Prediction Center), an AMO index (Enfield et al. 2001), and Labrador Current (LC) volume transport data (1992–2003) (Han and Li 2004) to assess the influences of NAO, AMO and LC variability on instrumental and shell-derived water temperatures in the GOM.

3 Results and discussion

3.1 Relationships between air temperatures, SSTs, and shell-derived water temperatures in the Western Gulf of Maine (GOM)

There is a significant relationship ($r = 0.59$; $P < 0.0001$) between annual air temperatures from Portland, Maine and the annual SST record at Boothbay Harbor from 1905 to 2003. Further, there is a relatively weak but statistically significant ($r = 0.33$; $P < 0.0003$) relationship between local air temperatures (Portland) and the shell-derived water temperature in the Western GOM during the same time interval. These results suggest that local air temperature in the GOM region are strongly linked to SST at Boothbay Harbor, and local air temperatures are weakly linked with water temperatures at 30 m in the Western GOM. However, it is difficult to determine if water temperatures are driving air temperatures along the coast, or if water temperatures are strongly influencing air temperatures.

A strong negative relationship ($r = -0.79$; $P < 0.0001$) exists between annual SST at Boothbay Harbor and the annual shell-derived $\delta^{18}O_c$ values in the Western GOM at 30 m water depth from 1905 to 2003. The robust relationship noted here demonstrates that shell $\delta^{18}O_c$ from *A. islandica* is a valid seawater temperature proxy. In order to calculate seawater temperatures from shell-derived $\delta^{18}O_c$ values the isotopic composition of the seawater ($\delta^{18}O_w$; related to salinity) must be known or estimated (see sect. 2.3 for details). After considering regional salinity/$\delta^{18}O_w$ changes, a comparison between annual SST at Boothbay Harbor and the annual shell-derived water temperature yielded a strong relationship ($r = 0.71$; $P < 0.0001$) in the Western GOM at 30 m water depth during 1905–2003 (Fig. 2). The correlations between the annual shell-derived water temperature record and seasonal SSTs at Boothbay Harbor are $r = 0.57$; $P < 0.0001$ (spring), $r = 0.49$; $P < 0.0001$ (summer), $r = 0.66$; $P < 0.0001$ (fall), and $r = 0.57$; $P < 0.0001$ (winter). It is interesting to note that the strength of correlations between the shell-derived annual water temperatures with seasonal SSTs at Boothbay Harbor are nearly equal. Further, the strongest correlation is between the annual shell-derived and annual SST record at Boothbay Harbor. Although there has been some debate about the length of the growing season for *A. islandica*, these results demonstrate that *A. islandica* appears to deposit shell aragonite nearly throughout the entire year, and thus we infer that there is not a substantial "shut-down" temperature (below ~6°C) previously described by Weidman et al. (1994). However, intra-annual shell $\delta^{18}O_c$ patterns do reveal an incomplete sinusoidal pattern, thus there is likely a period of "slow" growth in *A. islandica*. Recently, Schöne et al. (2005a), using high-resolution micromilling procedures (>1,050 carbonate samples in 38 years), concluded that one *A. islandica* specimen collected in Icelandic waters precipitated shell material in water temperatures ranging from 4.5 to 9.3°C, and the previously noted incomplete sinusoidal shell $\delta^{18}O_c$ pattern was present. Although more work is needed to better constrain "slow growth" periods in *A. islandica* with shell $\delta^{18}O_c$ patterns, based on the data presented here, the annually derived water temperatures from *A. islandica* do not appear to be biased to a particular season in the Western GOM. On average the SST at Boothbay Harbor is 2.2°C warmer than water temperatures at 30 m, which is consistent with recent buoy data (surface and at 20 m) from in the Western GOM. Shell-derived water temperatures (corrected for $\delta^{18}O_w$ —related to salinity) share ~50% variance with SSTs from Boothbay Harbor, suggesting that SSTs are a key factor influencing shell $\delta^{18}O_c$. The common variance between salinity and shell $\delta^{18}O_c$ values is less than 7% ($r = 0.26$; $P < 0.025$) from 1928 to 2003 (Fig. 2), indicating that salinity variations at 30 m in the Western GOM only impacted shell $\delta^{18}O_c$ in a minor way during the twentieth century. The remainder of the variance in the shell $\delta^{18}O_c$ record not explained by SSTs (at Boothbay Harbor) and 50 m salinity variations (at Prince 5) likely include analytical errors, and "local" effects from where the shells were collected (Fig. 1), which may not be captured by the Boothbay Harbor and Prince 5 records. Based on a comparison with SST at Boothbay Harbor, the shell-derived water temperature record (Fig. 2) illustrates the capability of *A. islandica* to accurately incorporate environmental variability on interannual-to-decadal timescales. This finding supports previous studies that used *A. islandica* to monitor basic hydrographic conditions (e.g., Weidman et al. 1994; Marsh et al. 1999; Schöne et al. 2004; 2005a, b, c). However, to

test if the strength of correlation is driven by long-term variations between the shell-derived water temperature record and SST record at Boothbay Harbor, we used a low-pass filter (Savitzky-Goley; window length = 5; second degree) to remove the high frequency bands from the shell-derived time series. We found that the annual correlation from 1905 to 2003 remained robust using this method ($r = 0.70$; $P < 0.0001$). We then subtracted the low-passed data from the original time series to isolate the high frequency bands (i.e. high-pass filter) and then compared the two time series again. This method yielded a relatively weaker correlation ($r = 0.44$; $P < 0.0001$) compared to the low-passed data. We conclude that the strength of the original correlation (Fig. 2) is primarily due to lower frequency components (near-decadal) of ocean variability, however high frequency components (interannual) contribute significantly to the overall correlation. This result offers insight into the mechanisms that may be driving water temperatures in the GOM.

3.2 NAO and AMO forcing of GOM water temperatures

The relationships between water temperatures in the GOM and the winter NAO and AMO are illustrated (Fig. 3). We used unsmoothed values for the winter NAO to assess the role of this climate mode on GOM water temperatures. The unsmoothed NAO correlations with GOM water temperatures were statistically significant with the highest correlations occurring with a 2-year lag (Fig. 3). Further, to assess decadal influences of North Atlantic SSTs on GOM water temperatures we used the AMO index of Enfield et al. (2001). Using this method, the AMO accounts for about 6–19 % (0 year lag) of water temperature variability

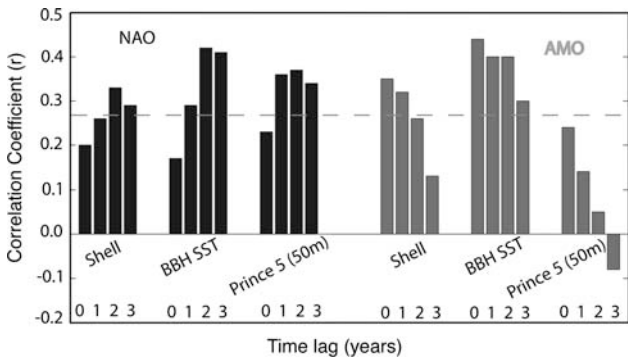

Fig. 3 Linear correlations between annual Gulf of Maine temperature records [Shell; *BBH* Boothbay Harbor; Prince 5 (50 m)] and dominant modes of North Atlantic climate [NAO (*black*) and AMO (*gray*)] with various lags from 1950 to 2003. *Gray dashed line* represents significance at the 95% confidence interval ($r > 0.26$)

in the GOM from 1950 to 2003, and the NAO accounts for approximately 11–18% (2-year lag) of water temperature variability during the same time interval (Fig. 3). Each of these climate modes separately influences water temperatures in the GOM, as the AMO and NAO are not correlated at a statistically significant level [$r = -0.18$ (no lag), $r = 0.05$ (1-year lag, AMO lags the NAO), $r = -0.09$ (2-year lag), $r = 0.01$ (3-year lag)]. Because the AMO index is a homogenized (0°–70°N) North Atlantic SST anomaly pattern the best correlation at each site location is without any temporal lag. However, the highest correlations between the NAO and GOM water temperatures occur with a 2-year lag. Changes in LC transport associated with the NAO take approximately 1.5–2 years to reach the GOM (see Drinkwater et al. 1999 for a detailed description). These results suggest that decadal patterns of the AMO and the NAO significantly impact water temperatures in the GOM. Although there is common variance between interannual water temperatures in the GOM and the NAO/AMO time series it is relatively low ($\sim$12–15%), thus other mechanisms must be primarily responsible for the shell-derived isotope record and water temperatures in the GOM since the 1950s. Although the impacts of the NAO and AMO are relatively minor, they are still important components in understanding regional climate forcing mechanisms in the GOM, especially on decadal time scales. We emphasize that we did not smooth either the NAO or AMO dataset, and this in part may explain the relatively low correspondence between GOM water temperatures with the NAO and AMO. The combined effects of the NAO and AMO modify GOM water temperatures on decadal-to-multidecadal timescales by modifying the relative amounts of each water mass (LSW and WSW) that enters the GOM. Persistent negative (positive) modes of the NAO and AMO would lead to colder (warmer) GOM water temperatures, thus changes in either of these climate modes during the late Holocene should be reflected by concurrent changes in the GOM.

Although there is not a clear dynamical link between the AMO and Gulf Stream activity, there is significant relationship ($r = 0.54$; $P < 0.001$) between the northernmost position of the Gulf Stream wall (Taylor and Stephens 1998) and the AMO index (Enfield et al. 2001) from 1966 to 1999, with the Gulf Stream position leading the AMO index by 4 years. This relationship merits further investigation, because hydrographic conditions in the GOM region are sensitive to the AMO and to changes in Gulf Stream activity (e.g., Petrie and Drinkwater 1993). Dima and Lohmann (2007) suggested that the positive phase of the AMO results from enhanced THC, which generates uniform positive SST anomalies in the North Atlantic. In the conceptual model of Dima and Lohmann (2007), SST increases in the North Atlantic are then followed by

decreased SLP in the North Atlantic and the multidecadal pattern is transferred in the Pacific via the tropics. Further, Dima and Lohmann (2007) claimed that an atmospheric teleconnection gives rise to a weakening Aleutian Low, and the resulting SLP fields in the North Atlantic and North Pacific enhance the export of Arctic sea ice and freshwater from the Fram Strait due to increased wind stress. The export of Arctic sea ice and freshwater into the North Atlantic would inhibit MOC, thus acting as a negative feedback mechanism regulating the phase of the AMO (Dima and Lohmann 2007). It is unclear if associated changes in MOC and associated feedbacks described by Dima and Lohmann (2007) would lead to modifications in the Gulf Stream properties (i.e. path or heat flux). This potential relationship may be important because, variability in Gulf Stream strength during the late Holocene may be linked to abrupt climate change in the North Atlantic (e.g., Lund et al. 2006; Lund and Curry 2006). The Gulf Stream is a great regulator of climate along the eastern North American coast because it transports $\sim$31 Sv of water in the Straits of Florida and exports $\sim 1.3 \times 10^{15}$ W of heat into the North Atlantic (Larsen 1992; Leaman et al. 1995; Baringer and Larsen 2001). Lund et al. (2006) concluded that the Gulf Stream transport in the Straits of Florida decreased during the Little Ice Age (LIA), and may in part be responsible for cooling in Europe. This seems to be consistent with previous work by Keigwin (1996) from the Sargasso Sea in the North Atlantic. In addition, recent studies (Keigwin et al. 2003; Marchitto and deMenocal 2003; Keigwin et al. 2005; Sachs 2007) have suggested that the slope and shelf waters in the Northwestern Atlantic have been cooling during the late Holocene, possibly related to THC variability and/or a southward migration of the Gulf Stream.

3.3 Shell-derived isotope record and reconstructed GOM water temperatures during the last millennium

The reconstructed water temperatures (using a fixed salinity) for intervals during the late Holocene from the Western GOM in 30–38 m of water are illustrated in Fig. 4a. The rationale for fixing salinity to reconstruct temperature prior to 1928 is based on the modern 75-year salinity mean (32.1 $\pm$ 0.22 PSU) at the Prince 5 (50 m) station, which shows no significant long-term trend (Fig. 2). Because shell $\delta^{18}O_c$ is a function of water temperature and the isotopic composition of the water ($\delta^{18}O_w$; related to salinity) (e.g., Epstein et al. 1953), we considered the possible effects of changing salinity assuming a constant water temperature. The reconstructed water salinities for intervals during the late Holocene from the Western

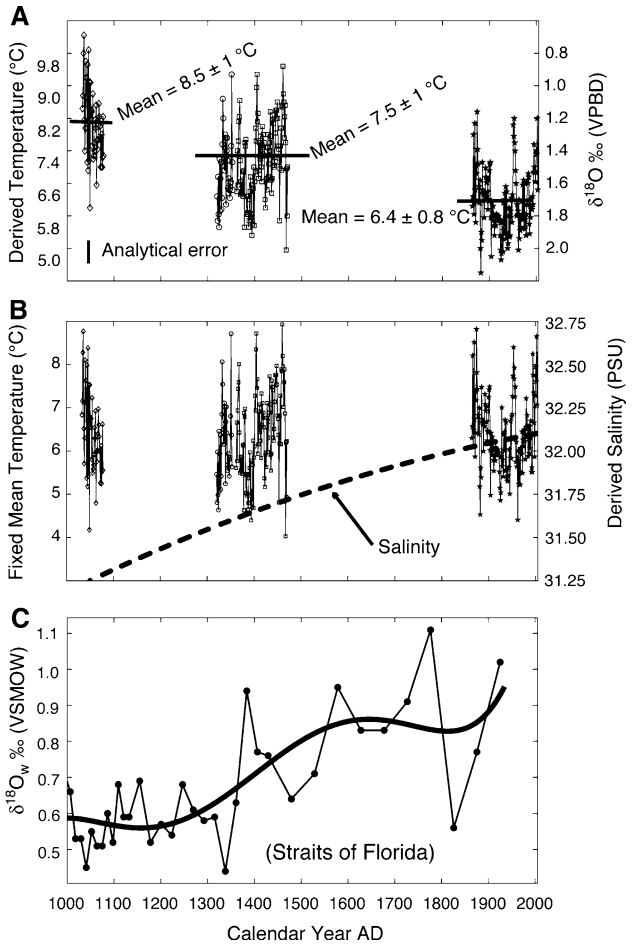

Fig. 4 **a** Late Holocene shell-derived water temperatures (after 1928; with long-term mean 50 m salinity values from Prince 5) and $\delta^{18}O_c$ record (indicates a maximum cooling), **b** and late Holocene shell-derived salinity values with fixed mean water temperatures (indicates a maximum salinity increase) are shown. The data in both **a** and **b** estimate maximum end-member conditions for the GOM. Long-term changes in $\delta^{18}O_w$ from the Florida Straits (Lund et al. 2006) are shown for comparison (**c**). We fit the Lund et al. (2006) data using a fifth order polynomial model to capture the rapid changes noted in $\delta^{18}O_w$ values. Higher $\delta^{18}O_w$ values would correspond to higher salinity values

GOM in 30–38 m of water are illustrated in Fig. 4b. Salinity values were calculated using the $\delta^{18}O_c$ long-term means for each of the intervals and fixing mean water temperatures. The salinity change during the record was modeled by a second-order polynomial (salinity = $[-4 \times 10^{-7} \times x^2 + 0.0022 \times x + 29.44]$) to estimate a gradual change in salinity. Alternatively the salinity change could have happened in a step-like function. Both the estimated temperature and salinity changes in Fig. 4a and b are maximum end-member conditions (cooling of 2°C or an increase in salinity of 0.82 PSU at 30 m). Although modern 50 m salinity values in the GOM are relatively constant at the Prince 5 station, we have no evidence to support that long-term changes in salinity did not occur

during the past millennium. Further, there were significant shifts in $\delta^{18}O_w$ during the last 1,000 years in the Florida Straits (Lund et al. 2006) (Fig. 4c), which may have impacted higher latitude $\delta^{18}O_w$ conditions. These noted shifts in $\delta^{18}O_w$ are important because water from the Florida Straits flows northward along the Eastern United States as the Gulf Stream and mixes outside the GOM with LSW. Unfortunately, the proxy records from the GOM and Florida Straits are not equivalently resolved. Therefore, changes in $\delta^{18}O_w$ conditions from the lower Gulf Stream can only be used qualitatively when estimating GOM water temperatures. Given the uncertainty associated with constraining $\delta^{18}O_w$ and salinity in the GOM during the last 1,000 years, we estimate that the Western GOM cooled by a maximum of 2°C. Alternatively, if the influence of Gulf Stream derived water (higher $\delta^{18}O_w$ and salinity values) was enhanced while the influence of LC derived water (lower $\delta^{18}O_w$ and salinity values) was diminished, then a reduced cooling (~1°C) and an increase in salinity (~0.4 PSU) would be possible in the GOM.

Using a fixed $\delta^{18}O_w$ /salinity model (Fig. 4a), mean annual water temperatures from 1030 to 1078 ± 78 AD (Medieval warm period) were 8.5°C (1 σ = 1.0°C) based on the 46-year mean of shell $\delta^{18}O_c$ = 1.24‰ (1 σ = 0.23‰). From 1321 to 1470 ± 45 AD (early Little Ice Age) mean annual water temperatures were 7.5°C (1 σ = 1.0°C) based on the combined 143-year mean of two shells $\delta^{18}O_c$ = 1.47‰ (1 σ = 0.23‰), while modern (1864–2003 AD) mean annual water temperatures were 6.4°C (1 σ = 0.8°C) based on the 140-year mean shell $\delta^{18}O_c$ = 1.71 (1 σ = 0.19‰) (Fig. 4a). Because the calibrated $^{14}C_{AMS}$ ages for two shells used in this study (1320 ± 45 AD; 1357 ± 40 AD) were so close, we used cross-matching techniques (sclerochronology) to determine if the two shells overlapped. This method yielded no significant correlation in growth histories between the two shells. Interannual variability of shell $\delta^{18}O_c$ from 1030 to 1078 ± 78 AD and 1321–1470 ± 45 AD was equal (1 σ = 0.23‰), and only slightly less during the modern record (1 σ = 0.19‰). This suggests that the forcing mechanisms controlling interannual oceanographic conditions for the GOM region have been relatively similar and persistent at least during these intervals.

3.4 Labrador Current influence on GOM water temperatures

The relationship between annually averaged LC transport (NE Track 096 [transect length = 243.6 km], Eastern Newfoundland Slope) (Fig. 1) and the shell-derived temperature with a 1-year lag is shown in Fig. 5. Labrador current transport variability at this location explains most

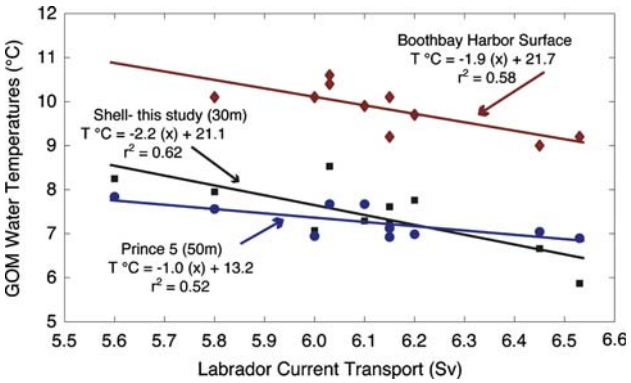

Fig. 5 The relationship between Labrador Current (LC) transport (Han and Li 2004) from the Eastern Newfoundland Slope (NE Track 096) (Fig. 1) and water temperatures in the Gulf of Maine (GOM) with a 1-year lag are shown. Shell isotope-derived temperatures (30 m) (*black filled squares* and *black line*; 1993–2003); Boothbay Harbor Surface (*red filled diamonds* and *solid red line*; 1994–2004); Prince 5 (50 m) (*blue filled circles* and *solid blue line*; 1993–2003). Each correlation between LC transport and water temperatures in the GOM is statistically significant ($r > 0.63$) at the 95% confidence interval

($r = -0.79$; $P < 0.007$) of the temperature variability at 30 m in the Western GOM from 1993 to 2003. In addition, LC transport variability explains ~51% ($r = -0.72$; $P < 0.019$; [1993–2003]) of the Prince 5 (50 m) water temperature record, and ~58 % ($r = -0.76$; $P < 0.011$; [1994–2004]) of SST variability at Boothbay Harbor with a 1-year lag (Fig. 5). The strength of the correlations, and the slopes between LC transport and GOM water temperatures are very similar for all three site locations, suggesting that LC transport modifies water temperatures in the entire GOM basin through deep water mixing processes. This result highlights the importance of LC variability on the modern oceanography in the GOM, and appears to be consistent with previously proposed mechanisms (e.g., Petrie and Drinkwater 1993; Drinkwater et al. 1999; MERCINA 2001; Loder et al. 2001). However, estimated LC transport data from locations along the Southern Newfoundland Slope [tracks 024 (transect length = 75.4 km), 113 (transect length = 98.6 km), and SW 096 (transect length = 69.6 km)] (Fig. 1), have substantially lower correlations [r = -0.19 (track 024), r = -0.25 (track 113), r = -0.44 (SW track 096)] with the GOM shell-derived water temperature record (with a 1-year lag) that are not statistically significant ($r > 0.63$; $P < 0.05$). The correlations are weak, because a substantial portion of the LC flows across the Grand Banks south of NE track 096 (see Han and Li 2004), thus these southerly transects do not fully capture primary LC variability. Using the modern and relatively short 10-year relationship between LC transport variability and the shell-derived and instrumental water temperatures in the GOM (Fig. 5), we tentatively propose

that either the LC cooled or LC transport increased during the late Holocene, resulting in an overall decrease in GOM water temperatures of 1–2°C. While the general $\delta^{18}O_c$ trend indicates decreasing water temperatures for the past 1,000 years, there are significant multi-decadal warming intervals throughout the record, most notably around 1400 AD and 1940 AD. This information is extremely valuable in assessing the natural range of water temperature variability in the GOM, and it appears that the recent warming (1940–present) (Fig. 2) is currently within the range of normal variability.

3.5 Independent evidence for late Holocene cooling in the Northwestern Atlantic based on multiple marine records

We compare our shell-derived water temperature record from the Western GOM with a select group of paleoceanographic records outside the GOM for the late Holocene (Fig. 6a). Marchitto and deMenocal (2003) showed a cooling of ~1°C of deep bottom water (1,854 m) from the Laurentian Slope, south of Newfoundland using Mg/Ca ratios derived from benthic foraminifera from ~900 AD to 1800 AD (Fig. 6b). Because the Mg/Ca ratio temperature estimations of Marchitto and deMenocal (2003) are independent of salinity values, they provide a relatively pure temperature signal. It is interesting to note that the deep bottom water site from the Laurentian Slope and the "relatively" shallow GOM site (Fig. 1) both show a similar magnitude cooling (Fig. 6a, b). Perhaps the observed cooling from both locations are dynamically linked. The GOM cooling trend is indicative a more negative NAO pattern during the late Holocene, and may have led to decreased Labrador Sea Water production, and increased LC flow. Although Marchitto and deMenocal (2003) suggested that either increased or decreased production of Labrador Sea Water could result in the noted cooling along the Laurentian Slope, there are other plausible hypotheses that may link the two sites in a mechanistic way. Decreased northern hemisphere summer insolation (e.g., Sachs 2007) during the Holocene may have cooled surface waters in the Labrador Sea, and thus water exported from the Labrador Sea was colder. Alternatively, a southward migration of the Gulf Stream during the late Holocene (Sachs 2007) and/or major changes in Gulf Stream transport (Lund et al. 2006) may explain the cooling from both locations.

The alkenone-based SST reconstruction of Keigwin et al. (2003) for Emerald Basin along the Scotian Shelf showed a cooling of ~0.8°C from ~400 to 1900 AD (Fig. 6c), which is likely a reflection of St. Lawrence outflow and possibly a minor contribution from the inshore

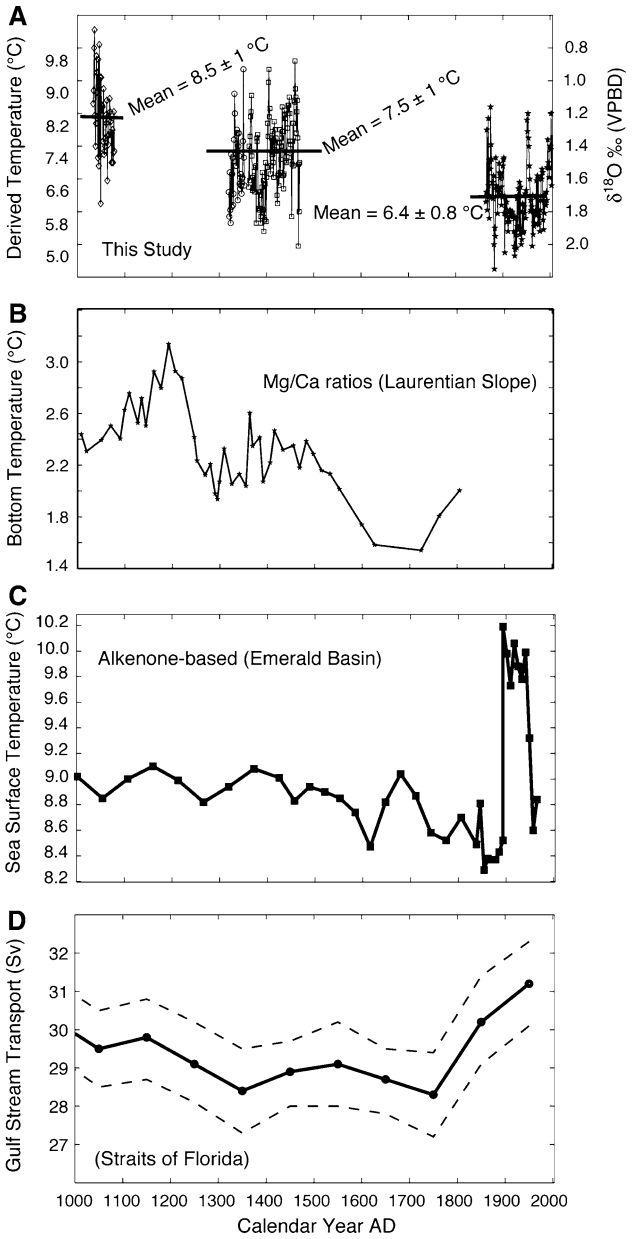

Fig. 6 **a** Late Holocene shell-derived $\delta^{18}O_c$ record and maximum water temperature change estimates are shown (Fig. 4a). **b** Part of the Mg/Ca ratio derived bottom water temperatures from the Laurentian Slope (1854 m) (Marchitto and deMenocal 2003), **c** part of the alkenone-based SST record (Keigwin et al. 2003) from Emerald Basin (Scotian Shelf), and **d** estimated Gulf Stream Transport in the Straits of Florida with 95% confidence intervals (*dashed lines*) (Lund et al. 2006) are shown for comparison

branch of the LC. The data of Keigwin et al. (2003) provide an independent measure of SST along the Scotian Shelf, which is fairly consistent with other marine-based studies in the region (e.g., Keigwin et al. 2005; Sachs 2007). Although there are considerable differences in the Emerald Basin and the GOM shell-derived water temperature records during the last century, sampling resolution and

data smoothing differences between the GOM and Emerald Basin records make comparing relatively short-term changes (decadal to centennial) problematic. A plausible explanation for the cooling noted in the GOM, Emerald Basin, and Laurentian Slope records (Fig. 6 [panels A, B, C]) during the last millennium may be due to large changes in the slope water properties. Proxy data by Lund et al. (2006) suggested that the transport of the relatively warm Gulf Stream water decreased by 2–3 Sv (6–10%) from ~1000 to 1800 AD (Fig. 6d). Thus a coupled increase of LC transport or LC cooling and a corresponding decrease in Gulf Stream-derived water (WSW) entering the GOM is a likely explanation of the shell-derived water temperature record from 1000 AD to the early 1900s. The general cooling trends during the last millennium are coincident with slowly decreasing Florida Straits transport estimates until ~1800 AD. Because we do not have any shell-derived temperature data ca. 1700–1850 AD (late Little Ice Age) in the GOM, we are unable to determine if GOM water temperatures were lower toward the end of the Little Ice Age compared to the modern shell-derived water temperature record (Fig. 2). From ~1900 to 1940 AD, SSTs at Boothbay Harbor and 30 m water temperature estimates from the shell-derived record (Fig. 2) indicate variable but non-trending water temperatures in the Western GOM. Both records from the Western GOM demonstrate a strong warming signal during the 1950s with a slight cooling in the early 1960s.

Keigwin et al. (2005) and Sachs (2007) concluded that slope waters in the Northwestern Atlantic have cooled dramatically (4–10°C) from Virginia to Nova Scotia during the Holocene possibly related to decreased summer solar insolation (at 65°N) or THC variability, specifically a southward migration of the Gulf Stream. Based on the marine proxy records (Fig. 6), we suggest that the LC cooled or LC transport increased and the influence of the Gulf Stream on GOM water temperatures during the late Holocene was diminished. We propose that slope water dynamics were the primary control on GOM water temperatures, with shell-derived water temperatures in 30–38 m of water in the Western GOM decreasing by 1–2°C during the last millennium.

4 Conclusions and future work

In this paper we present an annually resolved shell-derived $\delta^{18}O_c$ record in the Western GOM for intervals of the past 1,000 years that demonstrates major shifts in mean isotopic values likely related to slope water circulation. In either end-member configuration, the oceanic conditions in the Western GOM have changed considerably (maximum −2°C or +0.82 PSU at 30 m) during the late Holocene. Although the shell $\delta^{18}O_c$ record can be explained by changes in water temperature, $\delta^{18}O_w$ (related to salinity), or both, we believe that the most plausible explanation of the $\delta^{18}O_c$ record is represented by a cooling of GOM waters by 1–2°C during the past 1,000 years. The magnitude and rate of cooling in the GOM is consistent with other paleoceanographic estimates from regions located outside the GOM. A substantial portion (51–62%) of modern temperatures (with a 1-year lag) in the GOM are explained by LC transport variability along the Eastern Newfoundland Slope. We suggest that coupled slope water dynamics are the primary control on GOM water temperatures during the late Holocene. Specifically, we propose that LC transport increased or the LC cooled and the influence of the Gulf Stream on GOM water temperatures during the late Holocene was diminished. The NAO and AMO significantly impact interannual water temperatures in the GOM, however these modes explain less than 15% of the water temperature variability in the GOM since the 1950s. However, persistent modes of NAO or AMO may be more important on the oceanography in the GOM on decadal to centennial time scales. The inferred shell-derived cooling in the GOM during the last millennium is consistent with a persistent NAO negative mode. Over the last millennium, on decadal to centennial timescales water temperatures in the GOM primarily appear to reflect conditions in the North Atlantic. Future work will include independently constraining temperature or salinity conditions (e.g., alkenones, Sr/Ca ratios) in the Western GOM and developing a continuous shell-derived $\delta^{18}O_c$ record during the late Holocene to assess interannual-to-millennial scale oceanographic changes.

Acknowledgments We thank David Rodland and Sven Baier for their help preparing shell samples (INCREMENTS Research Group, University of Mainz), NOSAMS at Woods Hole Oceanographic Institution for AMS analyses, Association of Graduate Students (University of Maine) for travel support, Lloyd Keigwin, David Lund, and Thomas Marchitto for providing proxy data for Fig. 6, and Fei Chai (University of Maine) for helpful conversations that shaped this manuscript. North Atlantic Oscillation data were provided by National Oceanic and Atmospheric Administration (NOAA) (Climate Prediction Center; available at http://www.cpc.ncep.noaa.gov/data/teledoc/nao.shtml). Portland Maine air temperatures were provided by NOAA National Climate Data Center (available at http://www.ncdc.noaa.gov/oa/climate/research/cag3/me.html). Prince 5 station data were provided by Marine Environmental Data Services (Fisheries and Ocean Division of Canada; available at http://www.meds-sdmm.dfo-mpo.gc.ca/zmp/main_zmp_e.html). We thank Thomas Marchitto and an anonymous reviewer for providing constructive criticism and suggestions that substantially improved this manuscript. This study has been made possible in part by a German Research Foundation (DFG) grant (to BRS) within the framework of the Emmy Noether Program (SCH0793/1). This research was funded through the National Science Foundation (NSF ATM-0222553).

References

Baringer MO, Larsen JC (2001) Sixteen years of Florida Current transport at 27°N. Geophys Res Lett 28:3179–3182

Brown WS, Irish JD (1993) The annual variation of water mass structure in the Gulf of Maine: 1986–1987. J Mar Res 51:53–107

Cargnelli LM, Griesbach SJ, Packer DB, Weissberger E (1999) Essential fish habitat source document: Ocean quahog, *Arctica islandica*, life history and habitat characteristics. NOAA Technical Memorandum NMFS-NE-148, p 12

Conversi A, Piontkovski S, Hameed S (2001) Seasonal and interannual dynamics of *Calanus finmarchicus* in the Gulf of Maine (Northeastern US shelf) with reference to the North Atlantic Oscillation. Deep Sea Res II 48:519–530

Delworth TL, Mann ME (2000) Observed and simulated multidecadal variability in the Northern Hemisphere. Clim Dyn 16:661–676

Dickson R, Lazier J, Meincke J, Rhines P, Swift J (1996) Long-term coordinated changes in the convective activity of the North Atlantic. Prog Oceanogr 38:241–295

Dima M, Lohmann G (2007) A hemispheric mechanism for the Atlantic Multidecadal Oscillation. J Clim 20:2706–2719

Drinkwater KF, Belgrano A, Borja A, Conversi A, Edwards M, Greene CH, Ottersen G, Pershing AJ, Walker H (2003) The response of marine ecosystems to climate variability associated with the North Atlantic Oscillation. In: Hurrell J, Kushnir Y, Ottersen G, Visbeck M (eds) The North Atlantic Oscillation: climate significance and environmental impact, vol 134. AGU, Washington, pp 211–234

Drinkwater KF, Mountain DB, Herman A (1999) Variability in the slope water properties of eastern North America and their effects on adjacent shelves. ICES CM 1999/O:08, p 26

Enfield DB, Mestas-Nunez AM, Trimble PJ (2001) The Atlantic Multidecadal Oscillation and its relation to rainfall and river flows in the continental U.S. Geophys Res Lett 28:2077–2080

Epstein S, Buchsbaum R, Lowenstam HA, Urey HC (1953) Revised carbonate-water isotopic temperature scale. Bull Geol Soc Am 64:1315–1326

Folland CK, Palmer TN, Parker DE (1986) Sahel rainfall and worldwide sea temperatures. Nature 320:602–606

Forsythe GTW, Scourse JD, Harris I, Richardson CA, Jones P, Briffa K, Heinemeier J (2003) Towards an absolute chronology for the marine environment: the development of a 1000-year record from *Arctica islandica*. Geophysical Research Abstracts, Eur Geophys Soc 5

Gatien MG (1976) A study in the slope water region south of Halifax. J Fish Res Board Can 33:2213–2217

Goldenberg SB, Lansea CW, Mestas-Nunez AM, Gray WM (2001) The recent increase in Atlantic hurricane activity: causes and implications. Science 293:474–479

Greene CH, Pershing AJ (2003) The flip-side of the North Atlantic Oscillation and modal shifts in slope-water circulation patterns. Limnol Oceanogr 48:319–322

Grossman EL, Ku TL (1986) Oxygen and carbon isotope fractionation in biogenic aragonite: Temperature effects. Chem Geol 59:59–74

Han G, Li J (2004) Sea surface height and current variability on the Newfoundland slope from TOPEX/Poseidon Altimetry, Can. Tech. Rep. Hydrogr Ocean Sci 234 viii

Houghton RW, Fairbanks RG (2001) Water sources for Georges Bank. Deep Sea Res II 48:95–114

Hurrell JW (1995) Decadal trends in the North Atlantic Oscillation: regional temperatures and precipitation. Science 269:676–679

Jones DS (1983) Sclerochronology: reading the record of the molluscan shell. Am Sci 71:384–391

Keen MJ, Piper DJW (1990) Geological and historical perspective. In: Keen MJ, Williams GL (eds) Geology of the continental margin of eastern Canada, Vol I-1. Canadian Government Publishing Centre, Ottawa, pp 5–30

Keigwin LD (1996) The little ice age and medieval warm period in the Sargasso Sea. Science 274:1503–1508

Keigwin LD, Sachs JP, Rosenthal Y (2003) A 1600-year history of the Labrador current of Nova Scotia. Clim Dyn 21:53–62

Keigwin LD, Sachs JP, Rosenthal Y, Boyle EA (2005) The 8200 year B.P. event in the slope water system, western subpolar North Atlantic. Paleoceanography 20:doi:10.1029/2004PA001074

Knight JR, Allan RJ, Folland CK, Vellinga M, Mann ME (2005) A signature of persistent natural thermohaline circulation cycles in observed climate. Geophys Res Lett 32:doi:10.1029/2005GL024233

Knight JR, Folland CK, Scaife A (2006) Climate impacts of the Atlantic Multidecadal Oscillation. Geophys Res Lett 33, L17706, doi:1029/2006GL026242

Larsen JC (1992) Transport and heat flux of the Florida current at 27°N derived from cross-stream voltages and profiling data: theory and observations. Philos Trans R Soc Lond A 338:169–236

Lazier JRN, Wright DG (1993) Annual velocity variations in the Labrador Current. J Phys Oceanogr 23:659–678

Lazzari M (2001) Monthly and annual means of sea surface temperature: Boothbay Harbor, Maine 1905–2004

Leaman KD, Vertes PS, Atkinson LP, Lee TN, Hamilton P, Waddell E (1995) Transport, potential vorticity, and current/temperature structure across Northwest Providence and Santaren Channels and the Florida Current off Cay Sal Bank. J Geophys Res 100:8561–8569

Loder JW, Shore JA, Hannah CG, Petrie BD (2001) Decadal-scale hydrographic and circulation variability in the Scotia-Maine region. Deep Sea Res II 48:3–35

Lund DC, Curry W (2006) Florida Current surface temperature and salinity variability during the last millennium. Paleoceanography 21:doi: 10.1029/2005PA001218

Lund DC, Lynch-Stieglitz J, Curry WB (2006) Gulf Stream density structure and transport during the past millennium. Nature 444:601–604

Marchitto TM, deMenocal P (2003) Late Holocene variability of upper North Atlantic deep water temperature and salinity. Geochem Geophys Geosyst 4(12):1. doi:10.1029/2003GC000598

Marsh R, Petrie B, Weidman CR, Dickson RR, Loder JW, Hannah CG, Frank K, Drinkwater K (1999) The 1882 tilefish kill—a cold event in shelf waters off the north-eastern United States? Fish Oceanogr 8:39–49

MERCINA (2001) Oceanographic responses to climate in the Northwest Atlantic. Oceanography 14:76–82

Myers RA, Helbig J, Holland D (1989) Seasonal and interannual variability of the Labrador Current and West Greenland Current. ICES CM 16:18pp

Petrie B, Drinkwater K (1993) Temperature and salinity variability on the Scotian Shelf and in the Gulf of Maine. J Geophys Res 98:20,079–20,090

Petrie B, Yeats P (2000) Annual and interannual variability of nutrients and their estimated fluxes in the Scotian Shelf- Gulf of Maine region. Can J Fish Aquat Sci 57:2536–2546

Pettigrew NR, Townsend DW, Xue H, Wallinga JP, Brickley PJ, Hetland RD (1998) Observations of the Eastern Maine Coastal Current and its offshore extensions in 1994. J Geophys Res 103(30):623–639

Ropes JW, Jones DS, Murawski SA, Serchuck FM, Jearld A (1984) Documentation of annual growth lines in ocean quahogs, *Arctica islandica* Linne. Fish Bull 82:1–19

Ropes JW, Muraski SA (1983) Maximum shell length and longevity in ocean Quahogs, *A. islandica* Linné. ICES CM K 32:1–8

Sachs JP (2007) Cooling of Northwest Atlantic slope waters during the Holocene. Geophys Res Lett 34:L03609. doi:03610.01029/02006GL028495

Schöne BR, Freyre Castro AD, Fiebig J, Houk SD, Oschmann W, Kröncke I (2004) Sea surface water temperatures over the period 1884–1983 reconstructed from oxygen isotope ratios of a bivalve mollusk shell (*Arctica islandica*, southern North Sea). Palaeogeogr Palaeclimatol Palaeoecol 212:215–232

Schöne BR, Fiebig J, Pfeiffer M, Gleβ R, Hickson J, Johnson A, Dreyer W, Oschmann W (2005a) Climate records from a bivalve Methuselah (*Arctica islandica*, Mollusca; Iceland). Palaeogeogr Palaeclimatol Palaeoecol 228:130–148

Schöne BR, Houk S, Freyre Castro AD, Fiebig J, Oschmann W, Kröncke I, Dreyer W, Gosselck F (2005b) Daily growth rates in shells of *Arctica islandica*: assessing sub-seasonal environmental controls on a long-lived bivalve mollusk. Palaios 20:78–92

Schöne BR, Pfeiffer M, Pohlmann T, Siegismund F (2005c) A seasonally resolved bottom-water temperature record for the period AD 1866–2002 based on shells of *Arctica islandica* (Mollusca, North Sea). Int J Clim 25:947–962

Smith PC (1983) The mean and seasonal circulation off southwest Nova Scotia. J Phys Oceanogr 13:1034–1054

Stuiver M, Reimer PJ (1993) Extended 14C data base and revised CALIB 3.0 14C Age calibration program. Radiocarbon 35:215–230

Sutton RT, Hodson DLR (2003) Influence of the ocean on North Atlantic climate variability 1871–1999. J Clim 16:3296–3313

Sutton RT, Hodson DLR (2005) Atlantic Ocean forcing of North American and European summer climate. Science 309:115–118

Tanaka N, Monaghan MC, Turekian KW (1990) $\Delta^{14}C$ balance for the Gulf of Maine, Long Island Sound and the northern Middle Atlantic Bight: evidence for the extent of Antarctic intermediate water contribution. J Mar Res 48:75–87

Taylor AH, Stephens JA (1998) The North Atlantic Oscillation and the latitude of the Gulf Stream. Tellus 50:134–142

Thompson I, Jones DS, Dreibelbis D (1980) Annual internal growth banding and life history of the ocean quahog *Arctica islandica* (Mollusca: Bivalvia). Mar Biol 57:25–34

Weidman C, Jones GA, Lohmann KC (1994) The long-lived mollusk *Arctica islandica*: a new paleoceanographic tool for the reconstruction of bottom temperatures for the continental shelves of northern Atlantic Ocean. J Geophys Res 99:318,305–318,314

Weidman CR, Jones GA (1993) A shell-derived time history of bomb 14C on Georges Bank and its Labrador Sea implications. J Geophys Res 98:514,577–514,588